Accepted Manuscript

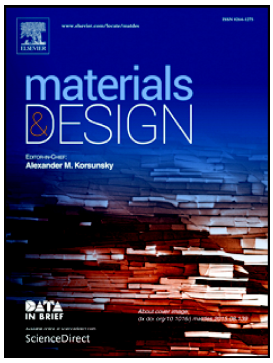

Intrinsic dead layer effects in relaxed epitaxial BaTiO3 thin film grown by pulsed laser deposition

Y. Gagou, J. Belhadi, B. Asbani, M. El Marssi, J-L Dellis, Yu. I. Yuzyuk, I.P. Raevski, J.F Scott

PII: S0264-1275(17)30237-X
DOI: doi: 10.1016/j.matdes.2017.03.001
Reference: JMADE 2835

To appear in: *Materials & Design*

Received date: 16 October 2016
Revised date: 28 February 2017
Accepted date: 1 March 2017

Please cite this article as: Y. Gagou, J. Belhadi, B. Asbani, M. El Marssi, J-L Dellis, Yu. I. Yuzyuk, I.P. Raevski, J.F Scott , Intrinsic dead layer effects in relaxed epitaxial BaTiO3 thin film grown by pulsed laser deposition. The address for the corresponding author was captured as affiliation for all authors. Please check if appropriate. Jmade(2017), doi: 10.1016/j.matdes.2017.03.001

Intrinsic dead layer effects in relaxed epitaxial $BaTiO_3$ thin film grown by pulsed laser deposition

Y. Gagou[1], J. Belhadi[1], B. Asbani[1], M. El Marssi[1], J-L Dellis[1], Yu. I. Yuzyuk[2], I. P. Raevski[2] and J. F Scott[3].

[1]*Université de Picardie Jules Verne, LPMC, 33 rue Saint-Leu, F-80039 Amiens, France*
[2] *Southern Federal University, Faculty of Physics, Zorge 5, Rostov-on-Don 344090, Russia*
[3] *Depts. of Chemistry and Physics, St. Andrews University, St. Andrews, Scotland KY16 9ST*

Abstract

Epitaxial $BaTiO_3$ (BT) thin film of about 400 nm thickness was grown on $LaSr_{0.5}Co_{0.5}O_3$ (LSCO) coated (001)MgO using pulsed laser deposition. Ferroelectric properties of the BT thin film in Pt/BT/LSCO/MgO heterostructure capacitor configuration were investigated. Dynamic P-E hysteresis loops at room temperature showed ferroelectric behavior with P_s = 32 µC/cm², P_r =14 µC/cm² and E_c=65 kV/cm. Static C-V measurements confirmed reversible switching with a coercive field E_c = 15 kV/cm. Basing on a model taking into account an interface dead-layer we show that the capacitance-voltage "butterfly" loops imply only 25% switching of dipoles that inferred from dynamic polarization-field loops (~ 4 and ~16 kV/cm, respectively). Dielectric permittivity as a function of temperature revealed a first-order ferroelectric-to-paraelectric (FE-PE) phase transition in the BT film characterized by a maximum at T_C ~130°C. The very large (~126 K at 1 kHz) difference between T_C and the extrapolated Curie-Weiss temperature T_0 is attributed to the dead-layer effects.

Keywords: Dead layer, Ferroelectric, $BaTiO_3$, Epitaxial growth, Pulsed laser deposition

Corresponding author: yaovi.gagou@u-picardie.fr

1. Introduction

Ferroelectric (FE) behavior, domain structure and phase transition in BT (barium titanate) bulk material were initially reported by Wul [1]. Several papers were thereafter reported on BT showing the Curie temperature between 120°C and 130°C in the bulk crystal [2,3]. Generally speaking BT exhibits a rotation of polarization <*P*> from [001] to [011] to [111] with lowering temperature, but this is a time- and space-averaged <*P*>, not a static value, so the dynamics are more order-disorder than displacive, as first shown by Comes and Lambert in 1968-9 [2,4] via diffuse streaks in Laue data.

Ferroelectric ABO_3 perovskite thin films are widely studied experimentally and theoretically due to their attractive physical properties attractive for various applications in micro- and nano-electronics, photonics, electrocalorics, domain wall electronics, tunable microwave devices, memristors, gas sensors etc [5–15]. In recent years, guided by the search for environmentally-friendly lead –free materials, $BaTiO_3$ (BT) and its solid solutions have attracted much attention [16,17]. Of special interest are epitaxial thin films, because in such objects the so-called strain engineering can be used for tailoring their properties [17–22].

A Landau-Devonshire approach has been used to analyze ferroelastic and electrical behavior in epitaxial BT thin films [19,23]. An absence of the lower-temperature structural phase transition in BT thin films had been previously reported by Pertsev *et al.* in 2000 [24] and Tennes *et al*. in 2004 [25], who showed that doping BT by Sr in the perovskite A-site led to relaxor behavior, as reported also by Zembilgotov et *al.* in 2002 [18]. However, the physical properties of ferroelectric thin films, in particular the electrical properties, have been known strongly dependent on the film thickness, choice of substrate, electrodes and fabrication process [26,27]. Many papers reported on the degradation of functional properties of FE thin films that can be an obstacle for applications [28,29]. Indeed, reduced tunability and permittivity, large coercive fields, small values of remnant polarization and a more diffused

ferroelectric phase transition as compared to those in the corresponding bulk materials are often evidenced in ferroelectric thin films [30,31]. Considerable experimental and theoretical investigations were undertaken to understand the origin of degradation and of some abnormal FE properties in thin films, and various models have been discussed to explain this degradation [32,33]. However, these phenomena are still not well understood. Many authors suggested the existence of an interface layer with passive low permittivity called a "dead layer" at the electrode–ferroelectric interfaces [34]. These dead layers act electrically as parasitic capacitors in series with the interior of the ferroelectric film. As a result of this interfacial capacitance, the suppression of permittivity when the thickness of the films decreases (often by several orders of magnitude) may occur, which initially was thought to be due to the intrinsic size effect of dielectric polarization [29,35]. However, that interpretation is now known to be completely wrong; there are no true size effects down to about 3 nm thickness [35,36].

In the present work, we report on the structural, ferroelectric and dielectric properties of a relaxed ferroelectric BT thin film grown by pulsed laser deposition (PLD). Considering the Interface Capacitance Model (ICM), we discuss the interface layer effects on coercive fields, permittivity and Curie-Weiss temperature in the Pt/BT/LSCO/MgO heterostructure capacitor. By comparison, in bulk $BaTiO_3$ samples, $\Delta T = T_c - T_0$ is usually about 10 °C. For the studied BT film, an unusual value of Curie-Weiss temperature T_0 was found to be equal to 6 °C at 1 kHz that corresponds to a ΔT = 126 °C; this value is dependent upon the probe frequency, which usually is a characteristic of relaxors and can reach below-freezing temperature values for low frequencies [37].

2. Experimental details

The target used for PLD technique was a typical dense ceramics obtained from solid state reaction method. The BT thin film was grown from this target by PLD using a Lambda Physik excimer laser (λ = 248 nm) in a MECA 2000 UHV deposition chamber equipped with a furnace especially designed to heat substrates up to high temperatures. The laser beam was focused on the rotating target as 2 mm^2 spot corresponding to a fluency of 2 J/cm^2. A 100 nm LSCO conducting electrode layer was deposited on the *(001)*MgO substrate at 750 °C at a partial oxygen pressure of 0.2 mbar.

The BT thin film has been deposited under an oxygen pressure of 0.1 mbar at 750°C. The film thickness (~400 nm) was measured, based on X-ray Laue oscillations that were observed from BT ultra-thin films. The surface quality of the LSCO and BT layers was monitored using reflection high-energy electron diffraction (RHEED).

X-ray diffraction measurements were performed using a Siemens D5000 diffractometer with a monochromatic CuK_α radiation. The in-plane measurements were performed using a 4-circles D8 Discover diffractometer. Dielectric measurements were carried out by the means of a Solartron SI-1260 spectrometer in the frequency range between 10^2 and 10^6 Hz in the conventional metal-dielectric-metal configuration using LSCO layer as a bottom electrode and sputtered platinum as a top circular electrodes (0.5 mm in diameter).

The temperature was controlled using a Linkam TS-93 hot stage that allows a temperature stability of ± 0.1 K. The P-E hysteresis loops measurements were performed at a frequency of 10 kHz with a classical Tower-Sawyer circuit using a Tektronix TDS-3032B oscilloscope, and ac triangular voltage source. Raman spectra were recorded from BT film excited with the polarized light of an Ar^+ laser (λ =514.5nm) and analyzed using a single spectrometer (JobinYvon Model T64000) equipped with a charge coupled device. Polarized Raman spectra were recorded in both normal and side-view backscattering geometries using a microprobe

device that allows the incident light to be focused on the sample as a spot of about 1 μm in diameter. The BT film sample was precisely aligned with respect to the crystallographic axis of the MgO substrate: Z//[001]MgO, Y//[010]MgO, and X//[100]MgO. The polarized Raman spectra presented here were recorded in parallel (Y(ZZ)$\overline{Y}$ and Y(XX)$\overline{Y}$) and crossed (Y(XZ)$\overline{Y}$ and Z(XY)$\overline{Z}$) geometries in which the incident light is polarized in parallel and perpendicular to the scattered light polarization, respectively.

3. X-ray diffraction and Raman spectroscopy studies

X-ray diffraction pattern obtained from BT/LSCO/*(001)*MgO thin film (Fig.1(a)) showed a single phase characterized by the first and second order diffraction peaks for both BT and LSCO layers with no parasitic phases. The BT film was single phase and well oriented since only one series of peaks was observed within the detection limits of our instrument. The full width at half maximum (FWHM) value calculated for the *(200)* reflection of BT thin film was 0.12°. This value, is only three times larger than that obtained for *(002)*MgO substrate, and is coherent with the crystalline ordering. Moreover, the rocking curve recorded on *(200)BT* peak presented in the inset of Fig.1(a) shows a FWHM value of 0.7° which is close to that of MgO substrate (0.5°). This result confirms the good crystalline quality of BT thin film without any significant mosaicity. Furthermore, to confirm the epitaxial growth of BT thin film, we used an in-plane Schulz reflection method [38] with a 4-circle diffractometer. An off-axis scan was performed on the *(113)*BT line and is presented in Fig.1(b); it shows a regular 90° spacing in a total ϕ scan range of 0-360°. The presence of four symmetric peaks indicates the cube-on-cube epitaxial growth of the BT layer and confirms the in-plane alignment of BT film and MgO substrate. From Bragg law we have determined the out-of-plane lattice parameter of BT film that was found to be 4.010 Å, which is between the *a*- and *c*-BT-bulk lattice parameters.

To confirm the BT layer orientation we have used Raman spectroscopy which is a more sensitive method to confirm the *a*- or *c*-axis orientations of the film basing on the Raman selection rules. Figure 2 displays Room temperature polarized Raman spectra of BT film in normal and side-view backscattering geometries. The spectra recorded in parallel $Y(ZZ)\bar{Y}$ and $Y(XX)\bar{Y}$) geometries are identical but different from that recorded in perpendicular ($Y(XZ)\bar{Y}$ and $Z(XY)\bar{Z}$) geometries which proves the excellent single crystal quality of the BT film. According to the Raman selection rules, for a tetragonal ferroelectric BT (point group C_{4v}) with polar axis along Z (*c*-axis), no Raman-active modes are allowed in the spectra corresponding to $Z(XY)\bar{Z}$ geometry. The E modes are only allowed for α_{zx} and α_{zy} Raman activity tensor components while the A_1 and B_1 modes are allowed simultaneously for the α_{xx} and α_{yy}. The α_{zz} component of the Raman tensor involves A_1 phonons exclusively. The Raman spectrum obtained for our BT film in the normal backscattering geometry $Z(XY)\bar{Z}$ contains E modes and is similar to that recorded in side-view backscattering $Y(XZ)\bar{Y}$ geometry (Fig.2). Note that the observed intensity difference between the two spectra is due to the analyzed volume which is much larger in the side-view backscattering geometry. In addition, the non-polar B1 mode observed at 306 cm^{-1} in $Y(ZZ)\bar{Y}$ geometry should not be observed if the film contains only *c*-domains. These features mean that the film cannot have tetragonal *c*-domain symmetry and imply that the polar axis is parallel to the plane of the substrate. [39–41]

4. P-E and C-V measurements at room temperature

Dynamic P-E response of BT thin film was recorded with a classical Tower-Sawyer circuit, and the results are reported in Fig.3. This figure shows a clear ferroelectric character with an ideal hysteresis loop, which demonstrates good ferroelectric behavior with a saturated polarization $2P_s$ = 64 µC/cm², remnant polarization $2P_r$ = 28 µC/cm² and coercive field $2E_C$ =

130 kV/cm. The obtained values are in good agreement with those reported by Shimuta *et al*. [42] and Choudhury *et al.* [43]. In Fig.3 we present also the switching current for BT film characterized by a maximal value of 2.80 µA that corresponds to E_C.

Additional *C-V* measurements were performed for better understanding of the switching mechanism of dipoles and the results are presented in Fig.4. These experiments were performed in the dc-mode to highlight the ferroelectric response of the easily reversible dipoles [44] in BT thin film. Figure 4 confirms the good ferroelectric properties of the studied BT film by the electric bias dependence of real dielectric permittivity ε_r(E) curve and the integrated easily reversible polarization curve deduced from these data, using the relation:

$$P_{rev} = (1/S) \int C(V)dV \qquad (1)$$

where S is the electrode surface, $C(V)$ is the measured capacitance as a function of voltage, and $\int$ is the integral in the voltage range (from $-V_m$ to V_m), where V_m is the maximum voltage value.

The dielectric permittivity ε_r' was calculated using the relation:

$$\varepsilon_r' = C\, d/(\varepsilon_0 S), \qquad (2)$$

where d is the thickness of the film and ε_0 is the permittivity of vacuum. High permittivity of about 1300 is obtained at E_C=20 kV/cm in the *C-V* measurements (Fig.4). The obtained value $2P_{rs}$ = 1 µC/cm² for the remnant polarization in a static mode (easily reversible dipole response) is small, and its contribution to the total P_r can be neglected. This value was reported in the literature for PZT thin films to be of about one-third of the Pr values in P-E dynamic recording [44]. Recall that the tunability $\eta = (\varepsilon(0) - \varepsilon(E))/\varepsilon(0)$ value calculated for the BT thin film was 57% when the applied field is E=100 kV/cm, indicating that dipoles can switch without much constraint. That means also that BT thin film could be used for tunable microwave applications, since it presents high permittivity, low loss factor, good P-E response and tunability. However, high coercive field value obtained for BT film compared to BT bulk

material argues in favor of the presence of dead layers at interfaces, which are studied in the following section.

5. Temperature and frequency dependence of dielectric permittivity

Dielectric permittivity versus temperature measurements were performed on a Pt/BT/LSCO*/(001)*MgO heterostructure thin film in a cylindrical capacitance shape having a thickness of 400 nm and electrode surfaces of 0.025 mm².

Temperature dependence of the real dielectric permittivity and of the loss factor measured on heating at different frequencies are shown in Fig. 5. This figure shows a diffuse dielectric anomaly around 132 °C with a large dielectric permittivity peak value of 1700 at a frequency of 100 Hz. This behavior confirms a relaxed state of the studied BT thin film. Indeed, a higher value of FE-PE phase transition temperature (T_C) as compared to bulk BT is usually reported for a strained BT thin films deposited by PLD on $SrTiO_3$ (ST) substrates [45]. Trithaveesak et al. [46] also reported that coating the ST substrate by a 50 nm conducting SrRuO3 (SRO) electrode have led to a FE-PE phase transition temperature close to that of BT bulk material.

In our case the presence of the LSCO electrode layer appears to be a source of partial relaxation of epitaxial strain imposed by the MgO substrate, which leads to a T_C value very close to that of the BT bulk material (120-130°C). Furthermore, the thermal hysteresis width of the permittivity-temperature curve is 15°C, as shown in the inset of Fig.5 which is characteristic for the first-order phase transition. However, the Curie-Weiss temperature T_0 deduced from the Curie-Weiss law shifted to low temperatures and depended on frequency. Namely, T_0 varies from -11°C to 8°C when the signal frequency increases from 100 Hz to 10 kHz. Thus a large gap exists between the temperature of dielectric anomaly T_C and the Curie-Weiss temperature T_0. The frequency dependence is however not the same for capacitance *C(V,T,f)* curves and for polarization hysteresis *P(V,T,f)* curves.

The results obtained at different frequencies are summarized in Table 1. The abnormal temperature gap $\Delta T=T_C-T_0$ is larger at low frequencies. The presence of dielectric dispersion and the diffuse FE-PE phase transition can probably be attributed to the presence of oxygen vacancies responsible for space charge and/or to the presence of residual weak constraints related to PLD epitaxial growth. Both these factors are known to produce a relaxor-like dielectric behavior in thin films [37]. In addition, we observe in Fig. 5 a frequency dispersion of permittivity values; while the T_C value is the same for all frequencies hence not displaying a relaxor-like behavior. Therefore, to explain the dead layer effect, we use in this paper a simplified interface capacitance model method taking into account the effects of the interfaces between the layers in the Pt/BT/LSCO heterostructure and we compare our results with those obtained for similar compounds previously [47,48]. According to this model a frequency dispersion of permittivity values, especially at high frequencies may be attributed, at least partially, to a comparatively high resistance of the LSCO electrode [48]. Although the ferroelectric hysteresis loops in our BT thin film are quite good, the Curie-Weiss temperature extrapolated from dielectric measurements seems to depend strongly on frequency and it is shifted to low temperatures, far below T_C. This behavior is abnormal, that is why we focus our study on the phase transition behavior in this thin film, using an interface capacitance model.

Indeed, BT thin film should be considered in our case as heterostructure consisting of a series-connected substrate-interface-BT thin film, except that in our case the material presents no substantial relaxor effects. We studied the influence of the ε_I/d_I ratio (where d_I and ε_I are the thickness and the permittivity of the interface layer, respectively) on the dielectric behavior of the film and we describe completely the effects of the dielectric response perturbation in a self-consistent way. We have not neglected the value of ε_I/d_I, but we separated out its influence on the dielectric properties of the thin film itself, assuming that ε_I/d_I is temperature independent.

6. Series interface capacitance model

Our main question concerns the E_C value which seems to be much larger (E_C = 65 kV/cm), than that reported for a bulk BT single crystal (~1 kV/cm) [49]. Let us recall that theoretical approach on the coercive field of $BaTiO_3$ single-domain crystals was previously proposed by Janovec in 1958 [50]. However, such a great increases of E_C with decreasing thickness is known for most ferroelectrics and was described for almost 50 years via the Kay-Dunn model [35].

This measured E_C value can be attributed to the effects of the interface capacitance, since the stress effects are neglected, because the values of T_C, P_r and the real part of dielectric permittivity (ε_r'), to be normal. As was already mentioned above, the gap between T_C and T_0 is very large, though we deal with a relaxed and epitaxial BT thin film. These considerations guided us to focus our investigation on the role of interface layer capacitance in the ferroelectric response of the studied BT thin film.

The effects of a dead layer were taken into account in the P-E and C-V responses of the thin film considered as a heterostructure. This investigation can be used for every grown thin film to highlight the effective contribution of the thin film to the overall ferroelectric response. BT heterostructure was modeled as a series-connected tri-layer each with its own capacitance. Calling respectively, C_H, C_I and C_F the capacitance of the heterostructure, interface layer and BT ferroelectric layer, we can express the total capacitance as:

$$1/C_H = 1/C_I + 1/C_F, \qquad (3)$$

where each element is assumed to be a planar capacitance,

$$C = \varepsilon_0 \varepsilon_r S/d \qquad (4)$$

in which S is the electrode area; d, the layer thickness; ε_0, vacuum permittivity; and ε_r, relative permittivity of each layer.

This gives

$d_H/\varepsilon_H = d_F/\varepsilon_F + d_I/\varepsilon_I$ (5)

where d_H, d_F and d_I are the thickness of the heterostructure, of the BT layer and of the interface layer, respectively; and $d_H = d_I + d_F \cong d_F$, because the interfaces thickness $d_I << d_F$. Hence, the equation (5) could be expressed as reported by Tyunina et *al.* [48]:

$1/\varepsilon_H \cong 1/\varepsilon_F + d_I/(\varepsilon_I\, d_H) = 1/\varepsilon_F + (1/d_H)(d_I/\varepsilon_I)$ (6)

Previous studies of epitaxial thin films of different ferroelectrics grown on MgO substrates with LSCO bottom electrodes and with Pt top electrodes have shown that ε_I/d_I ratio can be considered temperature-independent at least within the -200 to 250 °C temperature range [48]. However, ε_I/d_I ratio depends on frequency. It is worth to note that we varied the ε_I/d_I value in order to obtain a $\Delta T = T_C - T_0$ close to that observed in BT bulk materials. The Curie-Weiss temperature obtained from equation (6) varied substantially as a function of ε_I/d_I and accordingly $\Delta T = T_C - T_0$ values varied from a very large gap (at the lowest T_0) to a small gap (at T_0 close to T_C). In Fig.6 we show the experimental $\varepsilon'_r(T)$ and $1/\varepsilon'_r(T)$ curves measured at 1 kHz and fitted by Curie-Weiss law (Fig.6(a)) and the similar dependences calculated in the frame of the Interface Capacitance Model using the tested values ε_I/d_I = 4, 5 and 6 nm^{-1} (Figs.6(b-d)). It was found out that for $\varepsilon_I/d_I > 6$ nm^{-1} the ΔT exceeds 30°C which is much larger than ΔT values observed for BT bulk (Fig.6(b)). For $\varepsilon_I/d_I < 4$ nm^{-1} the value of T_0 is higher than T_C leading to negative ΔT values and the permittivity maximum becomes much higher than those ever observed for BT single crystals (Fig.6(d)). The realistic simulation of ε_I/d_I was finally considered in the range from 4 to 6 nm^{-1}. The best value of ε_I/d_I was found to be about 5 nm^{-1} that corresponds to ΔT= 10°C and T_0 = 122°C, as in the case of bulk BT.

When taking into account the Maxwell equations of continuity at the interfaces, we can write $\varepsilon_F E_{nF} = \varepsilon_I E_{nI}$ for normal projection of applied electric field, and then :

$\varepsilon_F V_F/d_F = \varepsilon_I V_I/d_I$ (7)

where V_I is a voltage applied to the interface layer and V_F is a voltage applied to the BT layer. We assume that $V_H = V_I + V_F$ is the voltage applied to the heterostructure.

From relation (7) we deduced the effective voltage (V_F) applied to the ferroelectric layer as a function of V_H, the voltage applied to the heterostructure:

$$V_F = V_H / [(\varepsilon_F / d_F)(\varepsilon_I / d_I) + 1] \qquad (8)$$

This expression in the case of $\varepsilon_I/d_I = 5\ nm^{-1}$ permits us to calculate the circuit characteristic values in P-E and C-V measurements for the effective value of the voltage applied to the BT layer in this heterostructure. The coercive fields obtained in P-E and C-V measurements were estimated to be ~ 16 kV/cm and ~ 4 kV/cm, respectively. These results show that only about the quarter of the applied field value drops across the proper BT ferroelectric layer while the other 75% drops across the interface (dead layer) in this heterostructure.

7. Conclusion

Epitaxial BT thin film was grown on *(001)*MgO substrate coated with 100 nm LSCO conducting layer using pulsed laser deposition. The relaxed BT film presents a dielectric anomaly at T_C =132°C, as in the bulk BT material, with a dielectric permittivity maximum of 1700 at 100 Hz. Dielectric P-E and C-V measurements were performed to characterize the ferroelectric behavior of the BT thin film. An abnormal gap between T_C and extrapolated Curie-Weiss temperature T_0 exceeding 126 K at 1 kHz was revealed. This gap depends upon frequency and is attributed to an interfacial passive dead layer with permittivity ε_I and thickness d_I in this heterostructure. Using an interface capacitance model we highlight the contribution of this dead layer to the ferroelectric response of the heterostructure. The best-fit value of Curie-Weiss temperature (T_0=122°C) is obtained for the ε_I/d_I ratio of about 5 nm^{-1}. The effective values of the remnant polarization P_r and coercive field E_c imply that only 25% of the applied electric field actually drops across the ferroelectric film.

Acknowledgement:

MEM acknowledges a support from the Region of Haut de France and IPR the Ministry of Education and Science of the Russian Federation (research project 3.1649.2017/PP).

References

[1] B. Wul, Dielectric Constants of Some Titanates, Nature. 156 (1945) 480–480. doi:10.1038/156480a0.

[2] M. Lambert, R. Comes, The chain structure and phase transition of BaTiO3 and KNbO3, Solid State Commun. 7 (1969) 305–308. doi:10.1016/0038-1098(69)90406-2.

[3] B. Ravel, E.A. Stern, R.I. Vedrinskii, V. Kraizman, Local structure and the phase transitions of $BaTiO_3$, Ferroelectrics. 206 (1998) 407–430. doi:10.1080/00150199808009173.

[4] R. Comes, M. Lambert, A. Guinier, The chain structure of BaTiO3 and KNbO3, Solid State Commun. 6 (1968) 715–719. doi:10.1016/0038-1098(68)90571-1.

[5] L.W. Martin, A.M. Rappe, Thin-film ferroelectric materials and their applications, Nat. Rev. Mater. 2 (2016) 16087. doi:10.1038/natrevmats.2016.87.

[6] Z. Xing, H. Wang, B. Xu, G. Ma, Y. Huang, J. Kang, L. Zhu, Structural integrity and ferroelectric–piezoelectric properties of PbTiO3 coating prepared via supersonic plasma spraying, Mater. Des. 1980-2015. 62 (2014) 57–63. doi:10.1016/j.matdes.2014.04.077.

[7] Z. Zhou, C.C. Bowland, B.A. Patterson, M.H. Malakooti, H.A. Sodano, Conformal $BaTiO_3$ Films with High Piezoelectric Coupling through an Optimized Hydrothermal Synthesis, ACS Appl. Mater. Interfaces. 8 (2016) 21446–21453. doi:10.1021/acsami.6b05700.

[8] B. Bhatia, H. Cho, J. Karthik, J. Choi, D.G. Cahill, L.W. Martin, W.P. King, High Power Density Pyroelectric Energy Conversion in Nanometer-Thick $BaTiO_3$ Films, Nanoscale Microscale Thermophys. Eng. 20 (2016) 137–146. doi:10.1080/15567265.2016.1252820.

[9] M. Tyunina, M. Savinov, Dynamic nonlinearity in epitaxial BaTi O 3 films, Phys. Rev. B. 94 (2016). doi:10.1103/PhysRevB.94.054109.

[10] Y. Heo, D. Kan, Y. Shimakawa, J. Seidel, Resistive switching properties of epitaxial $BaTiO_{3-\delta}$ thin films tuned by after-growth oxygen cooling pressure, Phys Chem Chem Phys. 18 (2016) 197–204. doi:10.1039/C5CP05333A.

[11] B. Allouche, Y. Gagou, F. Le Marrec, M.-A. Fremy, M. El Marssi, Bipolar resistive switching and substrate effect in GdK2Nb5O15 epitaxial thin films with tetragonal tungsten bronze type structure, Mater. Des. 112 (2016) 80–87. doi:10.1016/j.matdes.2016.09.047.

[12] S. Abel, T. Stoferle, C. Marchiori, D. Caimi, L. Czornomaz, M. Stuckelberger, M. Sousa, B.J. Offrein, J. Fompeyrine, A Hybrid Barium Titanate–Silicon Photonics Platform for Ultraefficient Electro-Optic Tuning, J. Light. Technol. 34 (2016) 1688–1693. doi:10.1109/JLT.2015.2510282.

[13] I. Gaponenko, P. Tückmantel, J. Karthik, L.W. Martin, P. Paruch, Towards reversible control of domain wall conduction in $Pb(Zr_{0.2}Ti_{0.8})O_3$ thin films, Appl. Phys. Lett. 106 (2015) 162902. doi:10.1063/1.4918762.

[14] S. Crossley, T. Usui, B. Nair, S. Kar-Narayan, X. Moya, S. Hirose, A. Ando, N.D. Mathur, Direct electrocaloric measurement of $0.9Pb(Mg_{1/3}Nb_{2/3})O_3$ -$0.1PbTiO_3$ films using scanning thermal microscopy, Appl. Phys. Lett. 108 (2016) 32902. doi:10.1063/1.4938758.

[15] M. Singh, B.C. Yadav, A. Ranjan, M. Kaur, S.K. Gupta, Synthesis and characterization of perovskite barium titanate thin film and its application as LPG sensor, Sens. Actuators B Chem. 241 (2017) 1170–1178. doi:10.1016/j.snb.2016.10.018.

[16] R. Su, D. Zhang, Y. Liu, J. Lu, Z. Wang, L. Li, J. Bian, M. Wu, X. Lou, Y. Yang, Novel lead-free ferroelectric film by ultra-small $Ba_{0.8}Sr_{0.2}TiO_3$ nanocubes assembled for a

large electrocaloric effect, Phys Chem Chem Phys. 18 (2016) 29033–29040. doi:10.1039/C6CP05462E.
[17] L. Mazet, S.M. Yang, S.V. Kalinin, S. Schamm-Chardon, C. Dubourdieu, A review of molecular beam epitaxy of ferroelectric $BaTiO_3$ films on Si, Ge and GaAs substrates and their applications, Sci. Technol. Adv. Mater. 16 (2015) 36005. doi:10.1088/1468-6996/16/3/036005.
[18] A.G. Zembilgotov, N.A. Pertsev, H. Kohlstedt, R. Waser, Ultrathin epitaxial ferroelectric films grown on compressive substrates: Competition between the surface and strain effects, J. Appl. Phys. 91 (2002) 2247. doi:10.1063/1.1427406.
[19] P.-E. Janolin, A.S. Anokhin, Z. Gui, V.M. Mukhortov, Y.I. Golovko, N. Guiblin, S. Ravy, M. El Marssi, Y.I. Yuzyuk, L. Bellaiche, B. Dkhil, Strain engineering of perovskite thin films using a single substrate, J. Phys. Condens. Matter. 26 (2014) 292201. doi:10.1088/0953-8984/26/29/292201.
[20] H. Wu, X. Ma, Z. Zhang, J. Zeng, J. Wang, G. Chai, Effect of crystal orientation on the phase diagrams, dielectric and piezoelectric properties of epitaxial $BaTiO_3$ thin films, AIP Adv. 6 (2016) 15309. doi:10.1063/1.4940205.
[21] S. Datta, M. Rioult, D. Stanescu, H. Magnan, A. Barbier, Manipulating the ferroelectric polarization state of BaTiO3 thin films, Thin Solid Films. 607 (2016) 7–13. doi:10.1016/j.tsf.2016.03.059.
[22] R. Guo, L. Shen, H. Wang, Z. Lim, W. Lu, P. Yang, Ariando, A. Gruverman, T. Venkatesan, Y.P. Feng, J. Chen, Tailoring Self-Polarization of $BaTiO_3$ Thin Films by Interface Engineering and Flexoelectric Effect, Adv. Mater. Interfaces. 3 (2016) 1600737. doi:10.1002/admi.201600737.
[23] V.B. Shirokov, Y.I. Yuzyuk, B. Dkhil, V.V. Lemanov, Phenomenological theory of phase transitions in epitaxial Ba Ti O 3 thin films, Phys. Rev. B. 75 (2007). doi:10.1103/PhysRevB.75.224116.
[24] N.A. Pertsev, V.G. Koukhar, Polarization Instability in Polydomain Ferroelectric Epitaxial Thin Films and the Formation of Heterophase Structures, Phys. Rev. Lett. 84 (2000) 3722–3725. doi:10.1103/PhysRevLett.84.3722.
[25] D.A. Tenne, X.X. Xi, Y.L. Li, L.Q. Chen, A. Soukiassian, M.H. Zhu, A.R. James, J. Lettieri, D.G. Schlom, W. Tian, X.Q. Pan, Absence of low-temperature phase transitions in epitaxial BaTiO 3 thin films, Phys. Rev. B. 69 (2004). doi:10.1103/PhysRevB.69.174101.
[26] J.F. Scott, L. Kammerdiner, M. Parris, S. Traynor, V. Ottenbacher, A. Shawabkeh, W.F. Oliver, Switching kinetics of lead zirconate titanate submicron thin-film memories, J. Appl. Phys. 64 (1988) 787. doi:10.1063/1.341925.
[27] B. Liu, G. Liu, H. Feng, C. Wang, H. Yang, Y. Wang, Effect of oxygen vacancies on structural, electrical and magnetic properties of La0.67Sr0.33CoO3 thin films, Mater. Des. 89 (2016) 715–720. doi:10.1016/j.matdes.2015.10.034.
[28] B.T. Lee, C.S. Hwang, Influences of interfacial intrinsic low-dielectric layers on the dielectric properties of sputtered (Ba,Sr)TiO[sub 3] thin films, Appl. Phys. Lett. 77 (2000) 124. doi:10.1063/1.126897.
[29] H. Yang, N.A. Suvorova, M. Jain, B.S. Kang, Y. Li, M.E. Hawley, P.C. Dowden, R.F. DePaula, Q.X. Jia, C.J. Lu, Effective thickness and dielectric constant of interfacial layers of Pt/Bi[sub 3.15]Nd[sub 0.85]Ti[sub 3]O[sub 12]/SrRuO[sub 3] capacitors, Appl. Phys. Lett. 90 (2007) 232909. doi:10.1063/1.2746953.
[30] N.A. Pertsev, J. Rodríguez Contreras, V.G. Kukhar, B. Hermanns, H. Kohlstedt, R. Waser, Coercive field of ultrathin Pb(Zr[sub 0.52]Ti[sub 0.48])O[sub 3] epitaxial films, Appl. Phys. Lett. 83 (2003) 3356. doi:10.1063/1.1621731.

[31] D.J. Kim, J.Y. Jo, Y.S. Kim, Y.J. Chang, J.S. Lee, J.-G. Yoon, T.K. Song, T.W. Noh, Polarization Relaxation Induced by a Depolarization Field in Ultrathin Ferroelectric BaTiO 3 Capacitors, Phys. Rev. Lett. 95 (2005). doi:10.1103/PhysRevLett.95.237602.
[32] I. Stolichnov, A. Tagantsev, N. Setter, J.S. Cross, M. Tsukada, Control of leakage conduction of high-fatigue-endurance (Pb, La)(Zr, Ti)O[sub 3] film ferroelectric capacitors with Pt/SrRuO[sub 3] electrodes, Appl. Phys. Lett. 75 (1999) 1790. doi:10.1063/1.124821.
[33] L.J. Sinnamon, R.M. Bowman, J.M. Gregg, Investigation of dead-layer thickness in SrRuO[sub 3]/Ba[sub 0.5]Sr[sub 0.5]TiO[sub 3]/Au thin-film capacitors, Appl. Phys. Lett. 78 (2001) 1724. doi:10.1063/1.1356731.
[34] L.-W. Chang, M. Alexe, J.F. Scott, J.M. Gregg, Settling the "Dead Layer" Debate in Nanoscale Capacitors, Adv. Mater. 21 (2009) 4911–4914. doi:10.1002/adma.200901756.
[35] H.F. Kay, J.W. Dunn, Thickness dependence of the nucleation field of triglycine sulphate, Philos. Mag. 7 (1962) 2027–2034. doi:10.1080/14786436208214471.
[36] A. Lookman, R.M. Bowman, J.M. Gregg, J. Kut, S. Rios, M. Dawber, A. Ruediger, J.F. Scott, Thickness independence of true phase transition temperatures in barium strontium titanate films, J. Appl. Phys. 96 (2004) 555. doi:10.1063/1.1759084.
[37] Y.H. Gao, J. Yang, H. Shen, J.L. Sun, X.J. Meng, J.H. Chu, Evolution of multiple dielectric responses and relaxor-like behaviors in pure and nitrogen-ion-implanted (Ba, Sr)TiO $_3$ thin films, Appl. Phys. Lett. 104 (2014) 122902. doi:10.1063/1.4869477.
[38] L.G. Schulz, A Direct Method of Determining Preferred Orientation of a Flat Reflection Sample Using a Geiger Counter X-Ray Spectrometer, J. Appl. Phys. 20 (1949) 1030. doi:10.1063/1.1698268.
[39] J. Belhadi, M. El Marssi, Y. Gagou, Y.I. Yuzyuk, Y. El Mendili, I.P. Raevski, H. Bouyanfif, J. Wolfman, Highly constrained ferroelectric [BaTiO3](1−x)Λ/[BaZrO3]xΛ superlattices: X-ray diffraction and Raman spectroscopy, J. Appl. Phys. 116 (2014) 34108. doi:10.1063/1.4890513.
[40] Y.I. Yuzyuk, R.A. Sakhovoy, O.A. Maslova, V.B. Shirokov, I.N. Zakharchenko, J. Belhadi, M. El Marssi, Phase transitions in BaTiO3 thin films and BaTiO3/BaZrO3 superlattices, J. Appl. Phys. 116 (2014) 184102. doi:10.1063/1.4901207.
[41] M. El Marssi, Y. Gagou, J. Belhadi, F. De Guerville, Y.I. Yuzyuk, I.P. Raevski, Ferroelectric BaTiO3/BaZrO3 superlattices: X-ray diffraction, Raman spectroscopy, and polarization hysteresis loops, J. Appl. Phys. 108 (2010) 84104. doi:10.1063/1.3496620.
[42] T. Shimuta, O. Nakagawara, T. Makino, S. Arai, H. Tabata, T. Kawai, Enhancement of remanent polarization in epitaxial BaTiO[sub 3]/SrTiO[sub 3] superlattices with "asymmetric" structure, J. Appl. Phys. 91 (2002) 2290. doi:10.1063/1.1434547.
[43] P. Roy Choudhury, S.B. Krupanidhi, Constrained ferroelectricity in BaTiO[sub 3]/BaZrO[sub 3] superlattices, Appl. Phys. Lett. 92 (2008) 102903. doi:10.1063/1.2894185.
[44] D. Bolten, U. Böttger, R. Waser, Reversible and irreversible polarization processes in ferroelectric ceramics and thin films, J. Appl. Phys. 93 (2003) 1735. doi:10.1063/1.1535748.
[45] F. Bai, H. Zheng, H. Cao, L.E. Cross, R. Ramesh, J. Li, D. Viehland, Epitaxially induced high temperature (>900 K) cubic-tetragonal structural phase transition in BaTiO[sub 3] thin films, Appl. Phys. Lett. 85 (2004) 4109. doi:10.1063/1.1812579.
[46] O. Trithaveesak, J. Schubert, C. Buchal, Ferroelectric properties of epitaxial BaTiO3 thin films and heterostructures on different substrates, J. Appl. Phys. 98 (2005) 114101. doi:10.1063/1.2135891.

[47] D. Xiao, L. Meng, G. Yu, The effect of surface layer on the dielectric behavior of complex oxide thin films, Mater. Des. 24 (2003) 377–382. doi:10.1016/S0261-3069(03)00030-X.
[48] M. Tyunina, J. Levoska, Application of the interface capacitance model to thin-film relaxors and ferroelectrics, Appl. Phys. Lett. 88 (2006) 262904. doi:10.1063/1.2218321.
[49] H.H. Wieder, Ferroelectric Hysteresis in Barium Titanate Single Crystals, J. Appl. Phys. 26 (1955) 1479. doi:10.1063/1.1721934.
[50] V. Janovec, On the theory of the coercive field of single-domain crystals of BaTiO3, Czechoslov. J. Phys. 8 (1958) 3–15. doi:10.1007/BF01688741.

Figure and table captions

Fig. 1: (a) X-ray diffraction pattern recorded on BT thin film showing *(h00)* orientations out-of-the substrate plan view and (b) its ϕ_{scan} showing an epitaxial growth and regular tailoring in *(113)* direction. The inset in Fig.1(a) shows a rocking curve recorded on *(200)* BT peak.

Fig.2 : Room temperature Raman spectra of BT film recorded in parallel $Y(ZZ)\bar{Y}$ and $Y(XX)\bar{Y}$) and crossed $(Y(XZ)\bar{Y}$ and $Z(XY)\bar{Z})$ light polarization geometries.

Fig.3: P-E hysteresis loop and integrated switching current recorded for BT thin film in a dynamic mode using a Sawyer -Tower circuit.

Fig.4: ε_r' -E butterfly curve recorded for BT thin film in a static mode and its corresponding free reversible polarization.

Fig.5: Temperature dependencies of the real part of permittivity ε'_r and loss factor for BT thin film measured at several frequencies in the course of heating . The inset shows thermal hysteresis of the $\varepsilon'_r(T)$ curve confirming first order character of phase transition in the film studied.

Fig.6: Experimental $\varepsilon'_r(T)$ and $1/\varepsilon'_r(T)$ curves measured at 1 kHz and fitted by Curie-Weiss law (panel (a)) and similar dependencies calculated in the frame of the Interface Capacitance Model using different values of the ε_I/d_I ratio (panels (b-d)).

Table 1: Curie-Weiss temperature, temperature gap and Curie constant depicted from Curie-Weiss law.

Figures

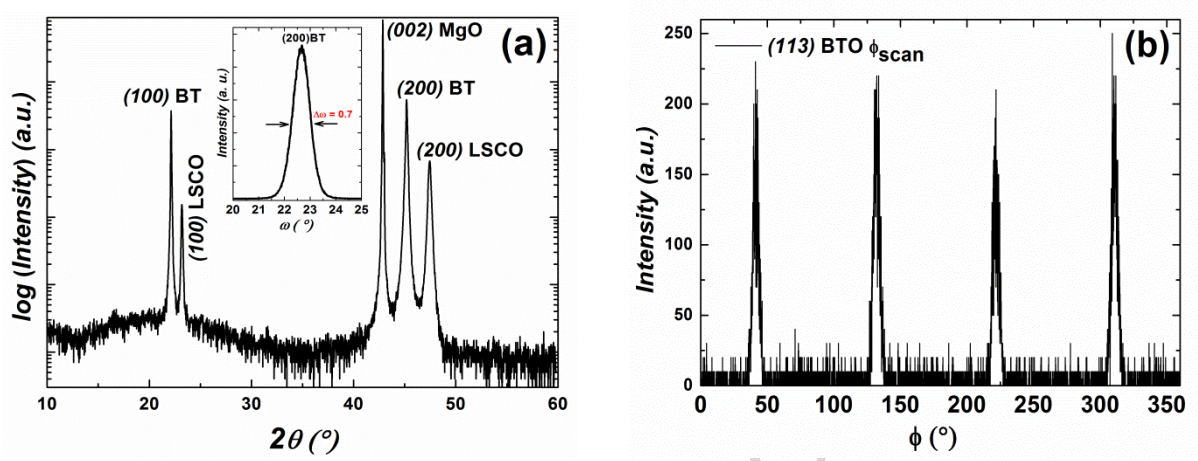

Fig. 1: (a) X-ray diffraction pattern recorded on BT thin film showing *(h00)* orientations out-of-the substrate plan view and (b) its ϕ_{scan} showing an epitaxial growth and regular tailoring in *(113)* direction. The inset in Fig.1(a) shows a rocking curve recorded on *(200)* BT peak.

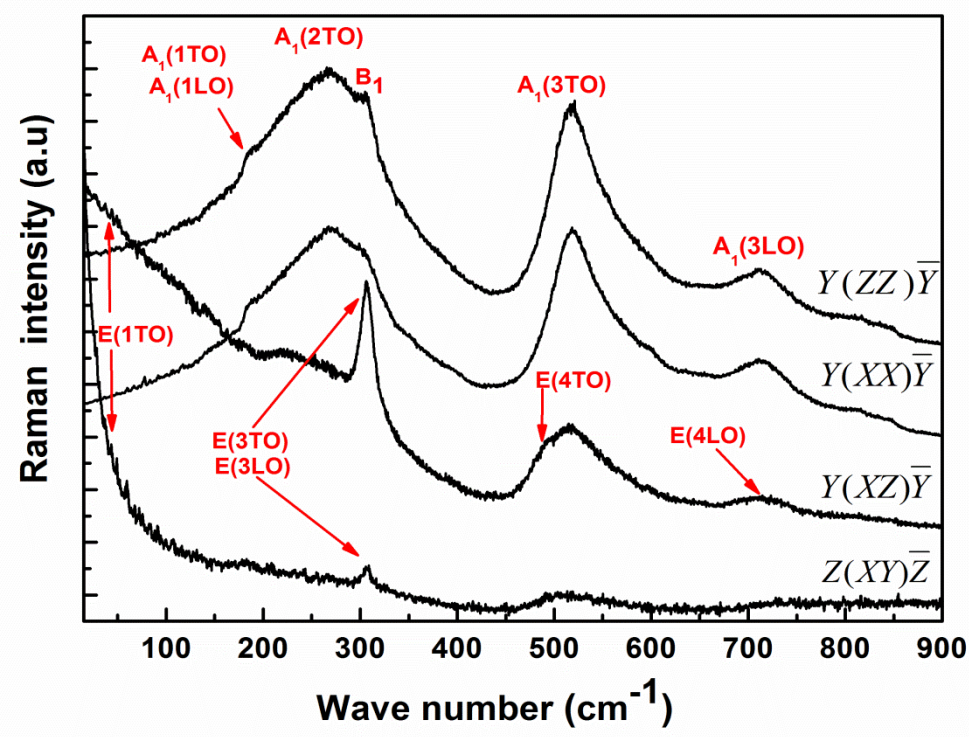

Fig.2 : Room temperature Raman spectra of BT film recorded in parallel (Y(ZZ)$\bar{Y}$ and Y(XX)$\bar{Y}$) and crossed (Y(XZ)$\bar{Y}$ and Z(XY)$\bar{Z}$) light polarization geometries.

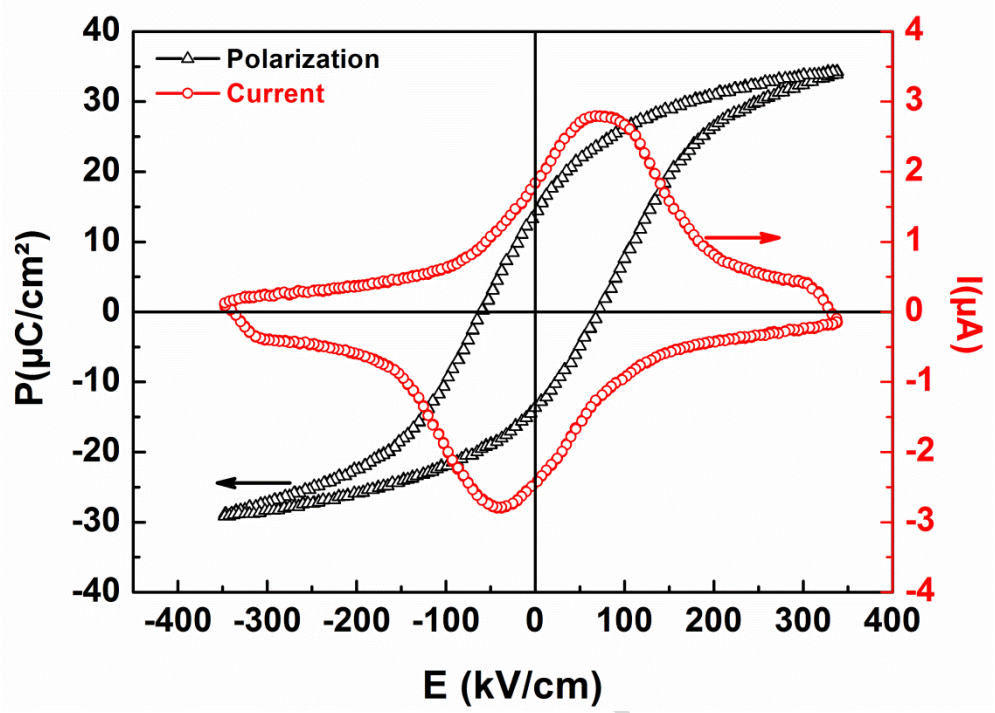

Fig.3: P-E hysteresis loop and integrated switching current recorded for BT thin film in a dynamic mode using a Sawyer -Tower circuit.

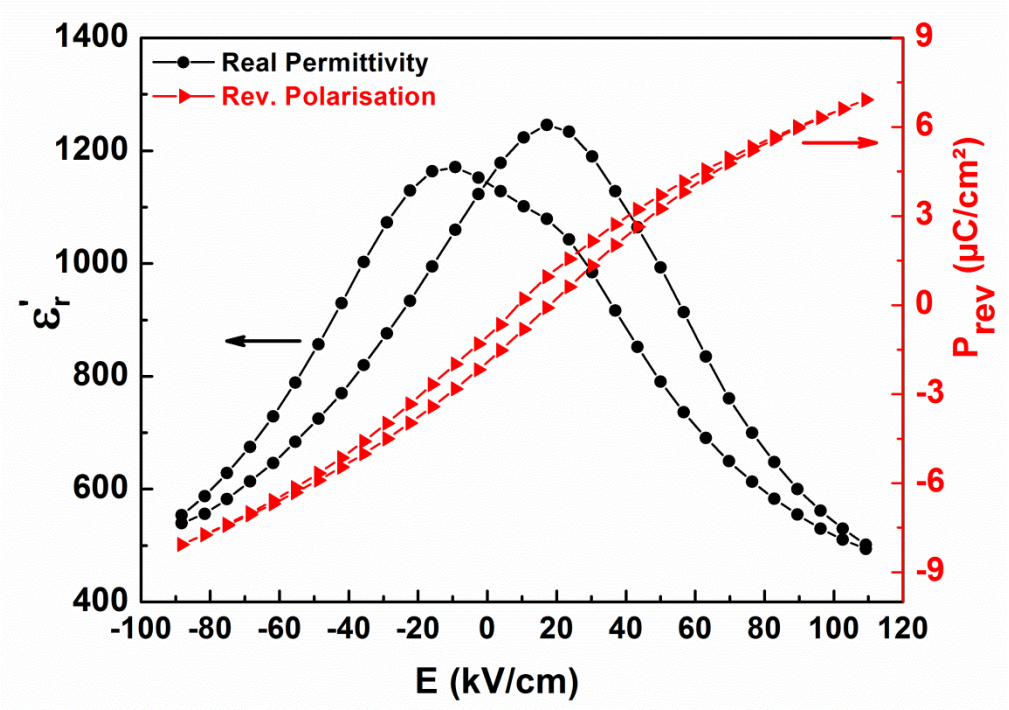

Fig.4: ε_r' -E butterfly curve recorded for BT thin film in a static mode and its corresponding free reversible polarization.

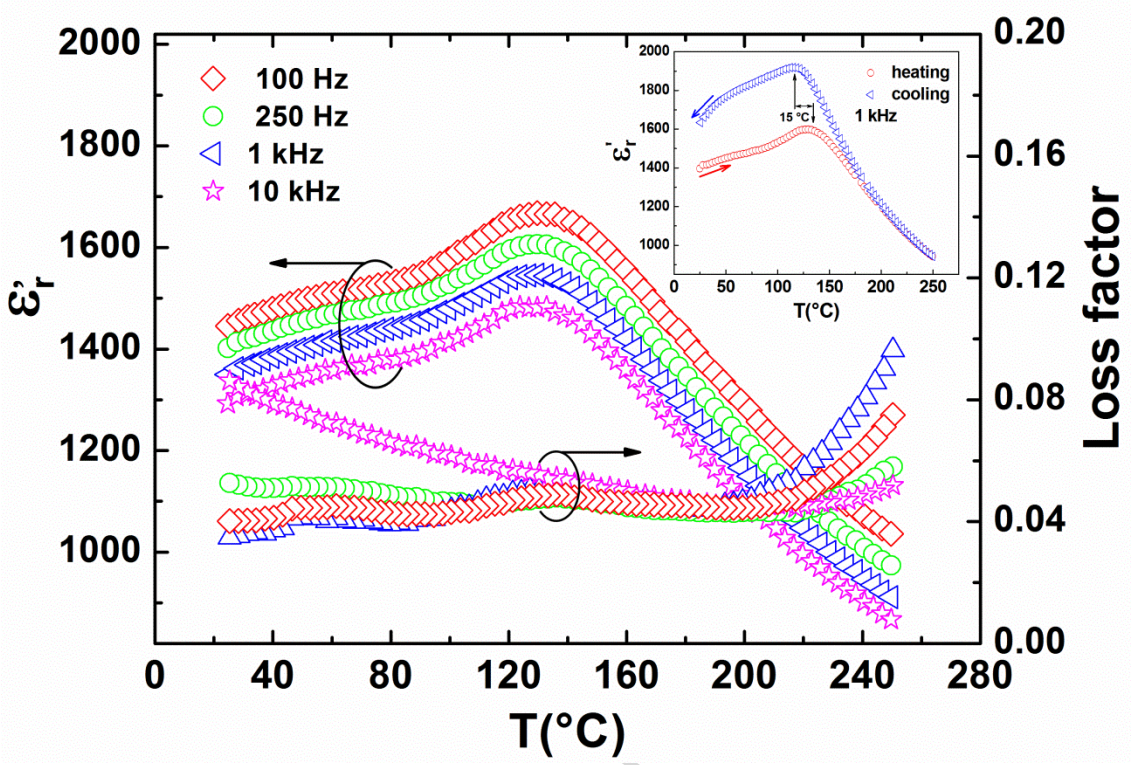

Fig.5: Temperature dependencies of the real part of permittivity ε'_r and loss factor for BT thin film measured at several frequencies in the course of heating . The inset shows thermal hysteresis of the $\varepsilon'_r(T)$ curve confirming first order character of phase transition in the film studied.

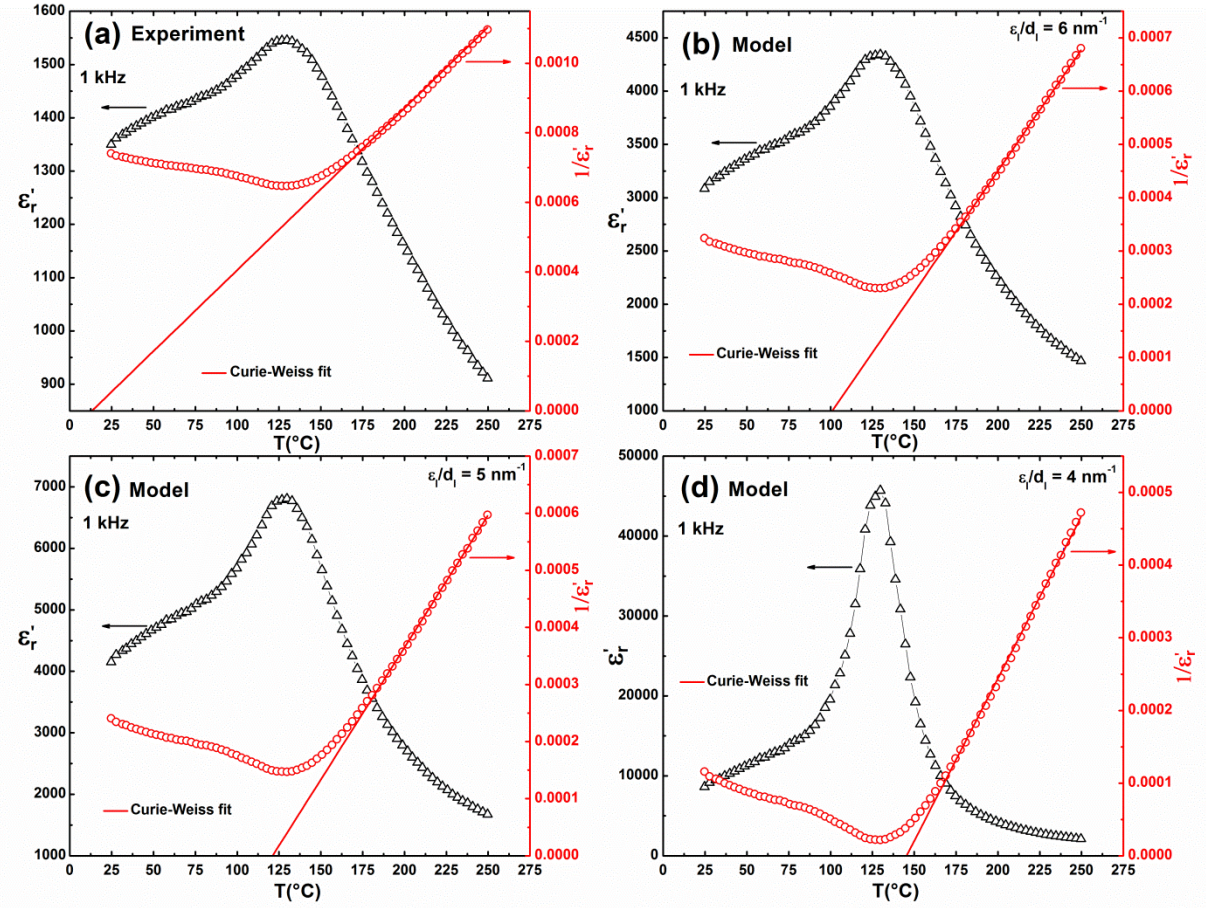

Fig.6: Experimental $\varepsilon'_r(T)$ and $1/\varepsilon'_r(T)$ curves measured at 1 kHz and fitted by Curie-Weiss law (panel (a)) and similar dependencies calculated in the frame of the Interface Capacitance Model using different values of the ε_I/d_I ratio (panels (b-d)).

Table

Table 1: Curie-Weiss temperature, temperature gap and Curie constant depicted from Curie-Weiss law.

Frequency	***T_0 (°C)***	***$\Delta T=T_C-T_0$ (°C)***	***$C\times 10^5$ (K)***
100 Hz	-11	143	2.70
200 Hz	-3	135	2.46
1 kHz	6	126	2.23
10 kHz	8	124	2.11

Graphical abstract

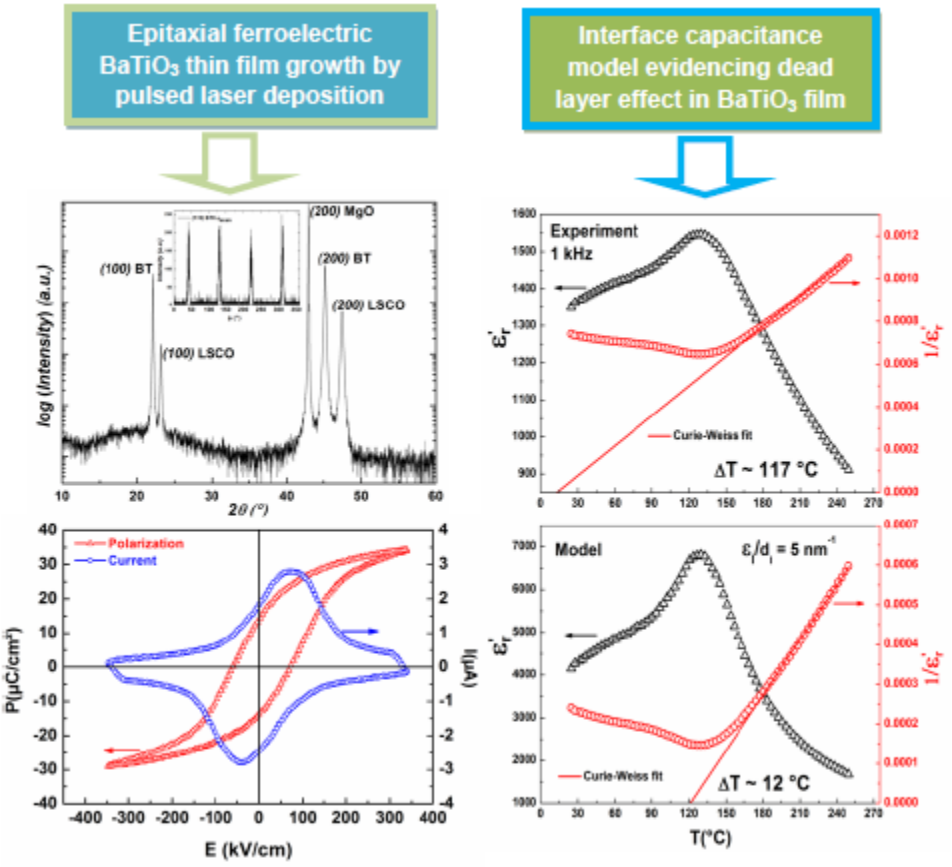

Highlights

- Epitaxial $BaTiO_3$ (BT) thin film of about 400 nm thickness was grown on (*001*)MgO coated $LaSr_{0.5}Co_{0.5}O_3$ (LSCO) by PLD techniques
- Fitted to a Curie-Weiss law, the calculated T_0 revealed an abnormal value, attributed to the dead-layer effects in ferroelectric response in BT film
- The effective ferroelectric characteristics P_r and E_c values imply that only 25% of the applied field actually drops across the ferroelectric film